

Coupling mode-destination accessibility with seismic risk assessment to identify at-risk communities

MAHALIA MILLER*

mahalia@alum.mit.edu

JACK W. BAKER†

bakerjw@stanford.edu

Abstract

In this paper, we develop a framework for coupling mode-destination accessibility with quantitative seismic risk assessment to identify communities at high risk for travel disruptions after an earthquake. Mode-destination accessibility measures the ability of people to reach destinations they desire. We use a probabilistic seismic risk assessment procedure, including a stochastic set of earthquake events, ground-motion intensity maps, damage maps, and realizations of traffic and accessibility impacts. For a case study of the San Francisco Bay Area, we couple our seismic risk framework with a practical activity-based traffic model. As a result, we quantify accessibility risk probabilistically by community and household type. We find that accessibility varies more strongly as a function of travelers' geographic location than as a function of their income class, and we identify particularly at-risk communities. We also observe that communities more conducive to local trips by foot or bike are predicted to be less impacted by losses in accessibility. This work shows the potential to link quantitative risk assessment methodologies with high-resolution travel models used by transportation planners. Quantitative risk metrics of this type should have great utility for planners working to reduce risk to a region's infrastructure systems.

Keywords. Infrastructure, Risk, Earthquakes, Transportation Network, Accessibility

1

I. INTRODUCTION

2 Seismic risk assessment in earthquake engineering tends to focus on buildings, bridges, and the
3 performance of infrastructure systems. For measuring the performance of transportation systems,
4 researchers typically use engineering-based metrics such as the post-earthquake connectivity loss,
5 which quantifies the decrease in the number of origins or generators connected to a destination
6 node [e.g., 1], or the post-earthquake travel distance between two locations of interest [e.g., 2].
7 These frameworks have provided insight into seismic vulnerability and possible risk mitigation,
8 but do not directly quantify ramifications for people.

9 In the field of vulnerability sciences, researchers have long stressed the importance of the
10 impact on human welfare from earthquakes. For example, Bolin and Stanford write that, "Natural"
11 disasters have more to do with the social, political, and economic aspects than they do with the
12 environmental hazards that trigger them. Disasters occur at the interface of vulnerable people
13 and hazardous environments" [3]. A recent World Bank and United Nations report echoed

*Corresponding author: Phone: +1-617-692-0574. Department of Civil and Environmental Engineering, Stanford University, 473 Via Ortega, MC 4020, Stanford, CA 94305, United States. Current address: Google, 345 Spear St., Floor 4, San Francisco, CA 94114, United States.

†Department of Civil and Environmental Engineering, Stanford University, 473 Via Ortega, MC 4020, Stanford, CA 94305, United States. URL: web.stanford.edu/~bakerjw/

this idea that the effects on human welfare turn natural hazards into disasters [4]. Historical events demonstrate the complex social effects of earthquakes. For example, on one hand the 1994 Northridge earthquake caused major damage to nine bridges, which, while significant, represented only 0.5% of the bridges estimated by Caltrans to have experienced significant shaking [5]. On the other hand, over half of businesses reported closing after the earthquake, with 56% citing the "inability of employees to get to work" as a reason [6]. Furthermore, the total economic cost of transport-related interruptions ("commuting, inhibited customer access, and shipping and supply disruptions") from this earthquake is estimated at 2.16 billion USD (2014) [7], using the consumer price index to account for inflation.

Some researchers have measured the impact of earthquakes on transportation infrastructure using the cumulative extra time needed for travel due to damage, sometimes called travel time delay [e.g., 8, 9]. This performance measure captures basic re-routing due to road closures and identifies roads more likely to be congested. Travel time approximately measures impact on people, but does not capture the fact that some destinations and trips have higher value than others. It also focuses on aggregate regional effects rather than individual communities and demographic groups. Others have considered the qualitative criteria-based metric "disruption index" [10], but this does not provide a quantitative link between physical damage to infrastructure and resulting human ramifications. Other work has looked at resiliency, but defined it in pure engineering terms, such as percentage of a road network that is functional [11]. Outside of transportation systems, some researchers have investigated the interplay between earthquake damage to the electric power and wastewater networks, and the usability of houses and other buildings [12].

In contrast to the work on transportation-related seismic risk, urban planning has a long tradition of studying the impact on people of events and policy [13]. Accessibility is one popular metric to measure the impact of different transportation network scenarios, and it measures how easily people can get to desirable destinations, which is one measure of social impact [14]. Within urban planning, accessibility has been measured in many ways, including individual accessibility, economic benefits of accessibility, and mode-destination accessibility [15]. The mode-destination accessibility is computed by taking the log value of the sum of a function of the utilities of each destination over all possible destinations and travel modes, where the utility decreases if getting to that destination is more costly or time-intensive [16]. This choice of accessibility definition is particularly useful for quantifying the impacts of disasters such as earthquakes, because certain destinations might be more critical for people in certain locations or from certain socio-economic groups. However, this accessibility measure has not previously been linked to risk assessment. In addition, the majority of work to date assumes that travel demand and mode choice will remain unchanged after a future earthquake, which historical data suggests is not the case [7]. A first step towards considering variable demand is work in the literature that varies demand by applying a constant multiplicative factor on all pre-earthquake travel demand [8], but again this approach lacks any resolution at the geographic or socio-economic level.

In this paper, we develop a framework for coupling mode-destination accessibility with a quantitative seismic-risk assessment to identify at-risk populations and measure the accompanying impacts on human welfare. We illustrate our approach with a case study of the San Francisco Bay Area transportation network, including highways, local roads, and public transportation lines. This study analyzes a set of forty hazard-consistent earthquake scenarios, ground-motion intensity maps, and damage maps, as introduced in [17, 18]. For each of these damage maps, we model damage with an agent-based transportation model used by the local transportation authorities that considers the impacts of damage to bridges, roads, and transit lines, and captures variable user demand. Then, with this model, we estimate losses in accessibility for 12 socio-economic groups and for a number of communities within the study region. The results provide a foundation

for evaluating risk mitigation actions, by utilizing a complete stochastic description of potential disaster impacts, rather than a set of impacts that is dependent upon a selected disaster scenario. Additionally, because the accessibility losses are associated with occurrence rates of the earthquake scenarios, the results are amenable to cost-benefit analyses of risk mitigation actions.

II. CASE STUDY: SAN FRANCISCO BAY AREA

We consider the San Francisco Bay Area to illustrate our approach (Figure 1). This seismically active area follows a polycentric metropolitan form, with San Francisco as the primary center and other jobs concentrated in suburban centers such as San Jose [19]. The region has a wide array of trip patterns for mandatory and non-mandatory trips. Furthermore, trip times and routes vary greatly depending on travel preferences and workplace locations [19]. Thus, there may be noticeable disparities among households in the risk of travel-related impacts due to earthquakes.

This analysis considers the complex web of roads and transit networks of the case study area. The roads are modeled by a directed graph $G = (V, E)$, where V is a finite set of vertices representing intersections, and the set E , whose elements are edges representing road links, is a binary relation on V . In this model, $(|V|, |E|) = (11,921, 32,858)$ including centroidal links and $(|V|, |E|) = (9,635, 24,404)$ without. Centroidal links do not correspond to particular physical roads but instead capture flows of people from outside the study area or from some minor local roads. Forty-three transit networks such as bus, light rail and ferry systems are also modeled. We model potential damage to 1743 highway bridges impacting the road and some transit networks, and 1409 structures impacting the rapid transit network, BART. Details of the seismic risk calculations for this network are provided in the following subsections.

I. Ground-motion intensity maps

I.1 Theory

We now describe how to produce a set of maps with ground-motion intensity realizations at each location of interest, and corresponding occurrence rates that reasonably capture the joint distribution of the ground-motion intensity at all locations of interest throughout the region [e.g., 20]. First, we generate Q earthquake scenarios from a seismic source model, which specifies the rates at which earthquakes of various magnitudes, locations, and faulting types will occur. This set of earthquake scenarios is comparable to a stochastic event catalogue in the insurance industry.

Second, for each earthquake scenario in the seismic source model, we use an empirical ground-motion prediction equation (GMPE) to predict the log mean and standard deviation of a ground motion intensity measure at each location of interest. Then, for each of the Q earthquake scenarios, we sample b realizations of spatially correlated ground-motion intensity residual terms. The total log ground-motion intensity (Y) for a given realization is computed as

$$\ln Y_{ij} = \overline{\ln Y(M_j, R_{ij}, V_{s30,i}, \dots)} + \sigma_{ij}\epsilon_{ij} + \tau_j\eta_j \quad (1)$$

where $\overline{\ln Y(M_j, R_{ij}, V_{s30,i}, \dots)}$ is the predicted mean log ground motion intensity at location index i , given an earthquake of magnitude M_j at a distance of R_{ij} , observed at a site with average shear wave velocity down to 30m of $V_{s30,i}$. Variability in ground motion intensity about this mean value is represented by σ_{ij} and τ_j , the within- and between-event standard deviations, respectively, for earthquake scenarios at the index $q = 1, \dots, Q$. The index j indicates the ground-motion intensity map ($j = 1, \dots, m$ where $m = Q \times b$), ϵ_{ij} is a normalized within-event residual representing location-to-location variability and η_j is the normalized between-event residual. Both ϵ_{ij} and η_j

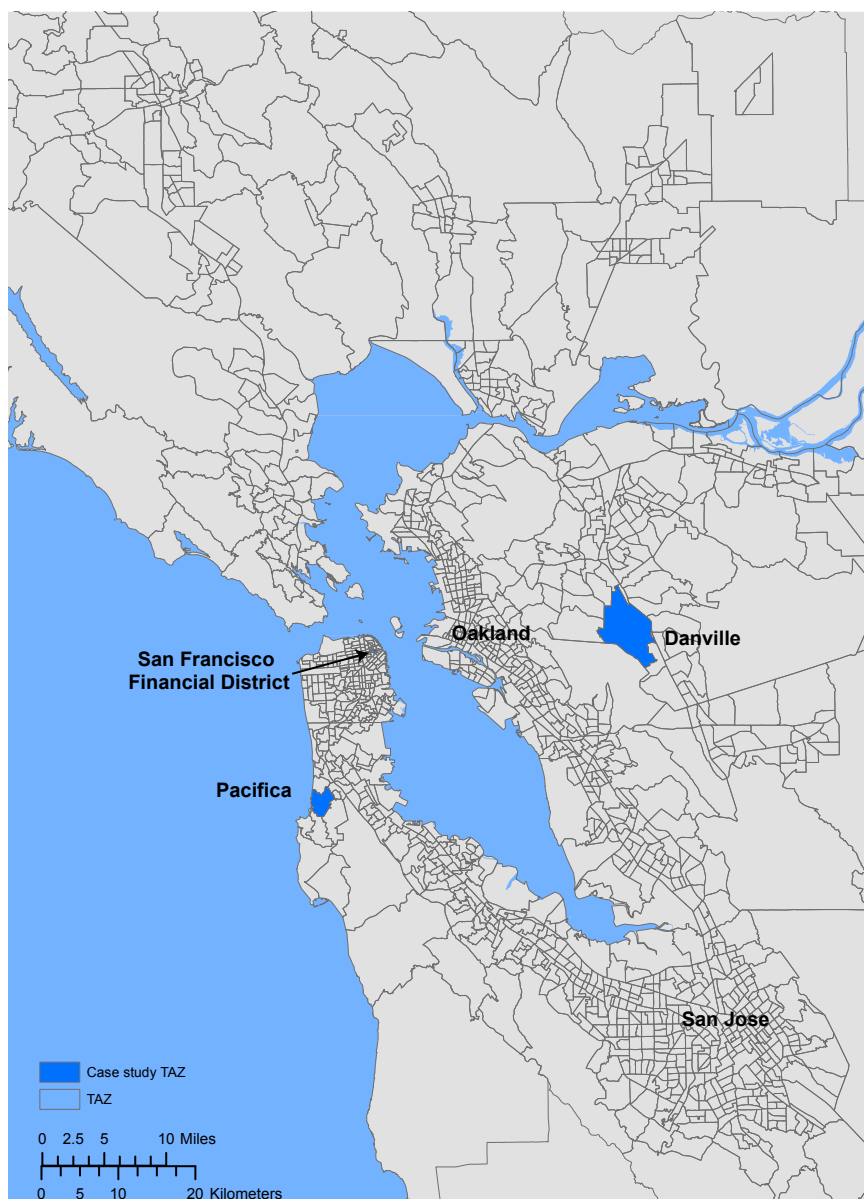


Figure 1: Travel analysis zones (TAZs) in the San Francisco Bay Area. Shading indicates the Danville, Pacifica and San Francisco Financial District TAZs that are considered in more detail below.

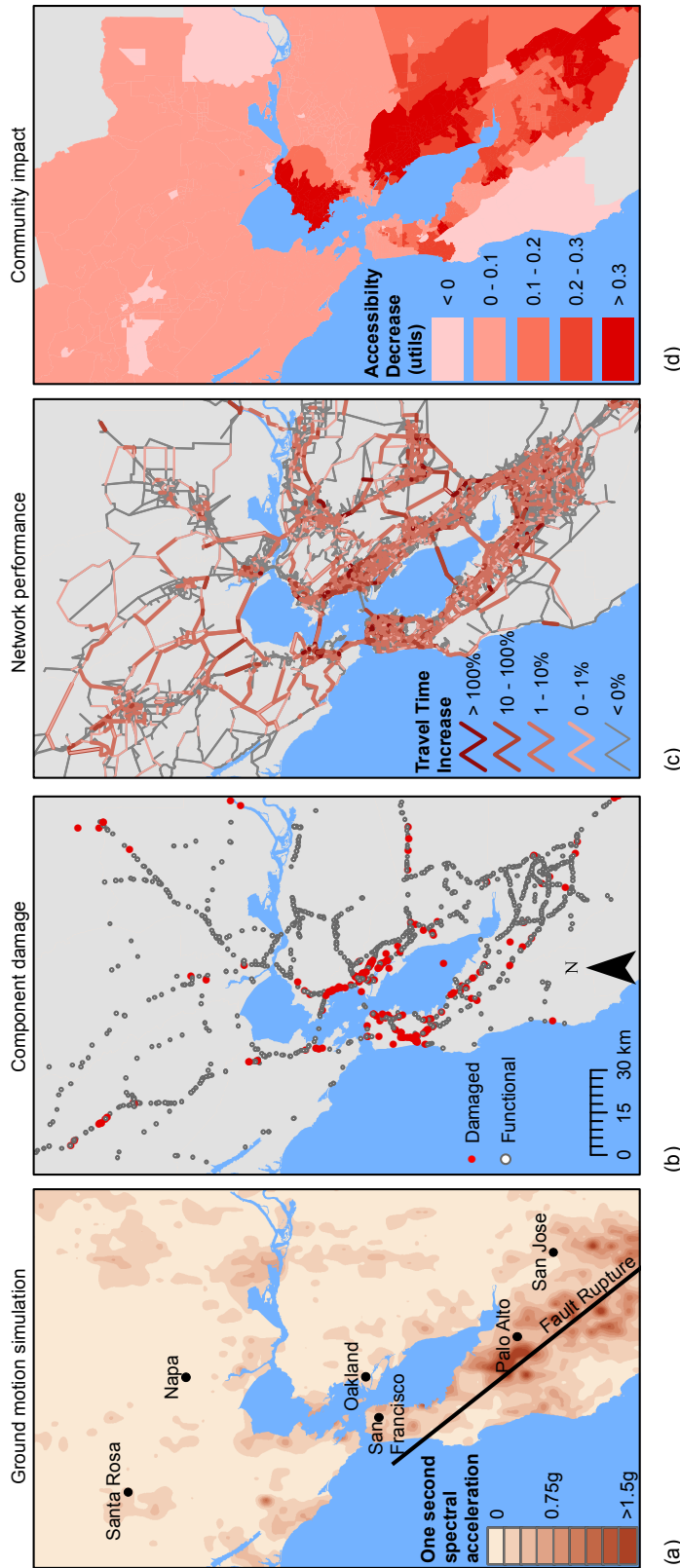


Figure 2: Illustration of the risk framework for one earthquake event including a) earthquake rupture and one-second spectral acceleration (ground motion intensity) map, b) bridge (component) damage map, c) map of travel time increase (network-performance measure) values and d) map of average accessibility decrease per travel analysis zone.

103 are normal random variables with zero mean and unit standard deviation. The vector of ϵ_{ij} has a
104 multivariate normal distribution and η_j is univariate.

105 The result is a set of m ground-motion intensity maps (e.g., Figure 2a). Since we simulate
106 an equal number (b) of ground-motion intensity maps per earthquake scenario, the annual rate
107 of occurrence for the j^{th} ground-motion intensity map is the original rate of occurrence of the
108 earthquake scenario, divided by b . We denote the occurrence rate of the j^{th} ground-motion
109 intensity map as w_j .

110 **I.2 Implementation**

111 To generate a stochastic catalog of ground-motion intensity maps, we use the OpenSHA Event Set
112 Calculator [21]. This software outputs the mean, \bar{Y}_{ij} , and standard deviation values, σ_{ij} and τ_j ,
113 for all locations of interest for a specified seismic source model and ground-motion prediction
114 equation, which are needed inputs for Equation 1. The intensity measure is the 5%-damped
115 pseudo absolute spectral acceleration (Sa) at a period $T = 1s$, which is the required input to the
116 fragility functions below. This spectral acceleration value represents the maximum acceleration
117 over time that a linear oscillator with 5% damping and a period of 1s will experience from a
118 given ground motion. We calculate these values at the location of each component (i.e., bridges
119 and other structures). Using one ground-motion intensity measure per component is a common
120 simplification that facilitates the use of fragility functions to easily predict damage to a given type
121 of structure [e.g., 9, 22]. We use the UCERF2 seismic source model to specify occurrence rates of
122 potential earthquakes in the region [23], the Wald and Allen topographic slope model to infer
123 $V_{s30,i}$ at each location [24], the Boore and Atkinson [25] ground-motion prediction equation and
124 the Jayaram and Baker model [26] for spatial correlation of ϵ_{ij} values.

125 **II. Damage maps**

126 **II.1 Theory**

127 The link between ground-motion intensity and damage to network components is provided by
128 fragility functions. Fragility functions express the probability $P(DS_i \geq ds_\zeta | Y_{ij} = y)$, where DS_i is a
129 discrete random variable representing the damage state for the i^{th} component and ds_ζ is a damage
130 state threshold of interest. The damage state is conditioned on the ground motion intensity
131 Y_{ij} having value y . We assume one component per location, and so identify both components
132 and locations via the index i . Researchers have calibrated fragility functions using historical
133 post-earthquake data [e.g., 27], experimental and analytical results [e.g., 28], hybrid approaches,
134 and expert opinion.

135 By sampling a damage state for each component, with probabilities obtained from the fragility
136 functions given the ground-motion intensity, we produce a damage map (e.g., Figure 2b). The
137 sampling process can be repeated to simulate multiple damage maps per ground-motion intensity
138 map. For example, if c damage maps are sampled per ground-motion intensity map, the occurrence
139 rates associated with the j^{th} damage map should be adjusted accordingly to $w_{j'}$, where $w_{j'} = w_j/c$,
140 and $j' = 1, \dots, J$.

141 *Functional percentage* relationships link the component damage to the functionality of network
142 elements. For example, in a road network, when a bridge collapses, the traffic flow capacity of the
143 road it carries and it crosses are reduced to zero. These relationships are typically derived from
144 a combination of observation and expert opinion, often due to data scarcity [29]. Furthermore,
145 the relationships are typically deterministic for a certain component damage state and restoration

146 time [29]. Thus, in this paper, each damage map corresponds to a functionality state for every
147 element of the network.

148 **II.2 Implementation**

149 **Component damage** We use fragility functions of the following form to provide the link between
150 ground-motion shaking and component damage:

$$P(DS_i \geq ds_\zeta | Y_{ij} = y) = \Phi\left(\frac{\ln y - \lambda_{\zeta,i}}{\xi_{\zeta,i}}\right), \quad (2)$$

151 where Φ is the standard normal cumulative distribution function, $\lambda_{\zeta,i}$ and $\xi_{\zeta,i}$ are respectively the
152 mean and standard deviation of the $\ln Y_{ij}$ value necessary to cause the ζ^{th} damage state to occur
153 or be exceeded for the i^{th} component, and the other variables are defined above.

154 The California Department of Transportation (Caltrans) provided the fragility function values
155 $\lambda_{\zeta,i}$ and $\xi_{\zeta,i}$ used for road bridges in this study [30]. The $\lambda_{\zeta,i}$ values are based on bridge
156 characteristics including number of spans and age [27], and the $\xi_{\zeta,i}$ values are constant for all
157 bridges. The BART seismic safety group provided the fragility function values $\lambda_{\zeta,i}$ and $\xi_{\zeta,i}$ used
158 in this study for the BART-related components [31]; data is available for the aerial structures,
159 primarily in the East Bay, but not tunnels. The BART fragility function values correspond to
160 the safety performance goals under the recent retrofit program, and both the $\lambda_{\zeta,i}$ and $\xi_{\zeta,i}$ vary
161 depending upon the structure's characteristics. Both sets of fragility functions are based on the
162 assumption that damage can be reasonably accurately estimated by the ground motion intensity
163 at each site independently, and that the damage state can be reasonably estimated by an analytical
164 model considering a single ground-motion intensity measure. In addition, the fragility curves
165 do not directly consider the effects of degradation. Current work is ongoing to refine these
166 assumptions [e.g., 28, 32, 33]. Per ground-motion intensity map, we sample one damage map (e.g.,
167 Figure 2b), which has a realization of the component damage state at each component location
168 according to the fragility function (eq. 2).

169 **Transit network damage** Each of the 43 transit systems we considered will function differently
170 when damaged. Because the Caltrain rail system consists of a single set of shared tracks, managers
171 suggested that the system would either be fully operational, or not at all if even one segment
172 of the system was non-operational. Similarly, managers suggested modeling the VTA system
173 as either fully or not at all functional. Depending on where the BART train cars are when the
174 earthquake strikes, the agency could accommodate different emergency plans. However, BART
175 representatives suggested that if any part of a route is damaged, the entire corresponding route
176 would not be operational (but other routes on different tracks might be still operational). In other
177 words, each BART route as well as the Caltrain and VTA routes are weakest-link systems, so the
178 failure of a single component will cause the route to be non-operational. We modeled the ferry
179 systems as fully functioning for all earthquake events. For all earthquake events including the
180 baseline, trans-bay and cross-county bus lines were discontinued, but main lines in urban areas as
181 well as other local bus networks were maintained per recommendations from the MTC (though
182 they face the same delays due to post-disaster traffic congestion as car travelers).

183 **Road network damage** The damage state of each Caltrans bridge maps directly to the traffic
184 capacity on associated road segments. Based on discussions with Caltrans, we consider travel
185 conditions one week after an earthquake, since it is a critical period for decision making (for exam-
186 ple, bridges would have been inspected and surface damage repaired, but major reconstruction

would not have yet begun). At this point in time, the components are assumed to have either zero or full traffic capacity [29]. We can thus summarize the component damage using two damage states, $ds_{damaged}$ (corresponding to HAZUS *extensive* or *complete* damage states) and $ds_{functional}$ (*none*, *slight*, or *moderate* damage states) [29]. Thus, the functional percentage relationship assigns zero traffic capacity on road segments that have at least one component in the $ds_{damaged}$ damage state, and full traffic capacity otherwise.

193 III. Network performance

194 III.1 Theory

195 The final step for the event-based risk analysis is to evaluate the network performance measure,
196 X . For this application, we consider mode-destination accessibility change [e.g., 15, 34, 35] (e.g.,
197 Figure 2d). Mode-destination accessibility, hereafter referred to as accessibility, measures the
198 distribution of travel destination opportunities weighted by the composite utility of all modes of
199 travel to those destinations (i.e., the ease of someone getting to different destinations weighted by
200 how desirable those destinations are) [16, 14]. The utility function for the mode-destination choice
201 may be estimated using a multinomial random utility model where the logsum represents the
202 accessibility value [36, 16, 14]. Namely, accessibility for a particular agent a is

$$Acc_a = \ln \left[\sum_{\forall \in C_a} \exp(V_{a(c)}) \right] \quad (3)$$

203 where $V_{a(c)}$ is the utility of the c^{th} choice for the a^{th} person, and C_a is the choice set for the a^{th}
204 person [16]. Choices refer to travel destinations and the mode of travel (driving, walking, bus, etc.).
205 The units are a dimensionless quantity, *utils*, but can be converted into equivalent time and dollar
206 amounts using *compensating variation* for cost-benefit studies. For the case study, 1 *util* equals
207 the value of 75 minutes or \$20 per person per day [14, 37, 38, 39]. With nearly 7 million people
208 in the study region, even small changes in average *utils* lead to large economic impacts. Since
209 accessibility measures how easily people can get to the destinations they desire, it is a measure a
210 of human welfare [e.g., 14].

211 Once the accessibility network performance measure is computed for each damage map, we
212 aim to estimate the exceedance rate of different levels of performance. The annual rate, λ , of
213 exceeding some threshold of network performance is estimated by summing the occurrence rates
214 of all damage maps in which the performance measure exceeds the threshold:

$$\lambda_{X \geq x} = \sum_{j'=1}^J w_{j'} \mathbb{I}(X_{j'} \geq x) \quad (4)$$

215 where x is an accessibility value threshold of interest and $X_{j'}$ is the accessibility value realization
216 for the j'^{th} damage map. The variable $w_{j'}$ is the occurrence rate of the j'^{th} damage map. The
217 indicator function \mathbb{I} evaluates to 1 if the argument, $X_{j'} \geq x$, is true, and 0 otherwise. By evaluating
218 λ at different threshold values, we derive an exceedance curve. We note here that this simulation-
219 based framework has an additional advantage of facilitating consideration of model uncertainty.
220 Multiple models can be sampled at any step within the framework, and the weights for the
221 sampled outcome (and resulting accessibility calculation) can be adjusted to account for the weight
222 on the particular model used. In the current results, some steps such as the earthquake source
223 model, consider model uncertainty extensively, while others do not.

224 **III.2 Implementation**

225 We compute accessibility using *Travel Model One* (version 0.3), an activity-based model used by the
 226 Metropolitan Transportation Commission (MTC), the local metropolitan planning organization
 227 (MPO) [40]. It represents the full road network as well as the public transit networks, biking, and
 228 walking. The agents in the travel model simulation are people drawn from the Census Public
 229 Use Micro-Sample, and are differentiated by their age, gender, worker status, student status, and
 230 household factors such as income, number of workers, number of vehicles, number of children,
 231 and other demographic data [40, 38, 41, 43]. The utility, $V_{a(c)}$, of the c^{th} choice for the a^{th} person
 232 is a function of factors including travel time, travel cost (including tolls), origin and destination
 233 density, automobile ownership, destination topography, distance to transit, household size, age,
 234 and the traveler's value of time, which is sampled from lognormal distributions based on the
 235 person's income [?]. The mode choice set, C , is: drive alone, drive with one other passenger, drive
 236 with two other passengers, walk, bicycle, transit via walking, and transit via driving. This data
 237 was collected by the MTC from household travel surveys, on-board transit passenger surveys, and
 238 census information [43].

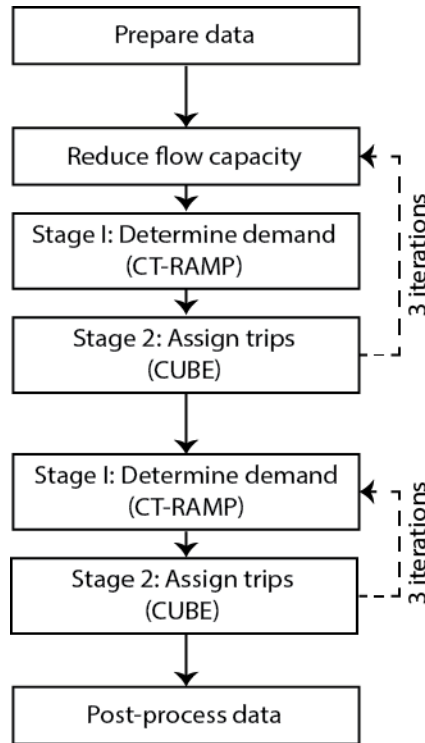


Figure 3: Analysis steps to evaluate travel demand and travel times.

239 We assume that the distributions of travel preferences do not change after an earthquake,
 240 although the actual destinations and trips will vary as people choose to forgo trips due to network
 241 disruption. The result is a variable-travel-demand model. This model uses a combination of
 242 Java code called CT-RAMP [42], and the Citilabs Cube Voyager and Cube Cluster transportation
 243 planning software [40]. The software takes 6+ hours on a high-performance computing platform to
 244 analyze a given network state, including reaching equilibrium on users trip choices and preferred
 245 travel modes and routes. Figure 3 illustrates the basic design of this variable-travel-demand model,

Table 1: Income class definitions for the case study region, as defined by the local planning organization, the MTC [38] and also translated to current 2014 USD using the consumer price index.

Income class	Income range, 1989 USD	Income range, 2014 USD
Low	< \$25,000	< \$47,334
Medium	\$25,000 - \$45,000	\$47,334 - \$85,202
High	\$45,000 - \$75,000	\$85,202 - \$142,004
Very high	> \$75,000	> \$142,004

246 where the "Determine demand" stage uses the utility functions described above among other
 247 factors, as implemented in the CT-RAMP module, and the "Assign trips" stage uses the Cube
 248 software. Readers are referred to [17] for a more detailed discussion of the model design.

249 Given the computational cost of analyzing the network, analyzing thousands of scenarios with
 250 a crude Monte Carlo approach is not feasible. This analysis uses an improved sampling strategy
 251 to select damaged networks for analysis, and considers 40 sets of ground-motion intensity maps,
 252 damage maps, accessibility performance measure realizations, and corresponding annual rates of
 253 occurrence. The 40 realizations were selected (and their occurrence rates adjusted appropriately)
 254 using optimization to ensure that the selected scenarios were consistent with the larger original
 255 set of simulations. Consistency was evaluated in terms of ensuring that the subset of maps had
 256 the same probability distributions of ground motion intensity at individual sites as the complete
 257 set of simulations, and that the distribution of the number of damaged bridges in the network
 258 is also consistent between the subset and full set. Because we ensure that these statistics of
 259 earthquake impacts are properly represented, we term the subset "hazard consistent," and infer
 260 that it will produce comparable probability distributions of accessibility impacts as the full set of
 261 simulations. Readers are referred to [17] for more details about this set of events and computing
 262 mode-destination accessibility using this model.

263 III. RESULTS AND DISCUSSION

264 I. Region-wide results

265 In this section, we analyze region-wide trends in accessibility losses for the case study area. We
 266 first analyze each of the 12 socio-economic groups used in practice for the case study region [38].
 267 These socio-economic groups correspond to all combinations of four income classes (Table 1), and
 268 three classes of automobile availability in the household (zero automobiles, fewer automobiles
 269 than household members that work, as many or more automobiles than household members that
 270 work). Each data point for analysis represents a trip by a person of a household from one of these
 271 segments, who is modeled as an agent in the transportation model. Expected losses are computed
 272 by taking an average of the accessibility losses for people within a given group and region for
 273 each earthquake event, weighted by the events' corresponding occurrence rates. Expected losses
 274 for people from each of the 12 groups and 1454 TAZs are shown in Figure 4.

275 In addition to looking at average accessibility loss, we can compute an accessibility exceedance
 276 curve for a given group or region. By using equation 4 to compute exceedance rates for multiple
 277 accessibility loss thresholds, we can produce results like those in Figure 5. These curves show, for
 278 a given group, the annual rate with which a given accessibility decrease will be observed (when
 279 considering random future occurrences of earthquakes and damage). Several observations can be
 280 made from these results.

281 First, a higher ratio of cars to the number of people who work in a household corresponds

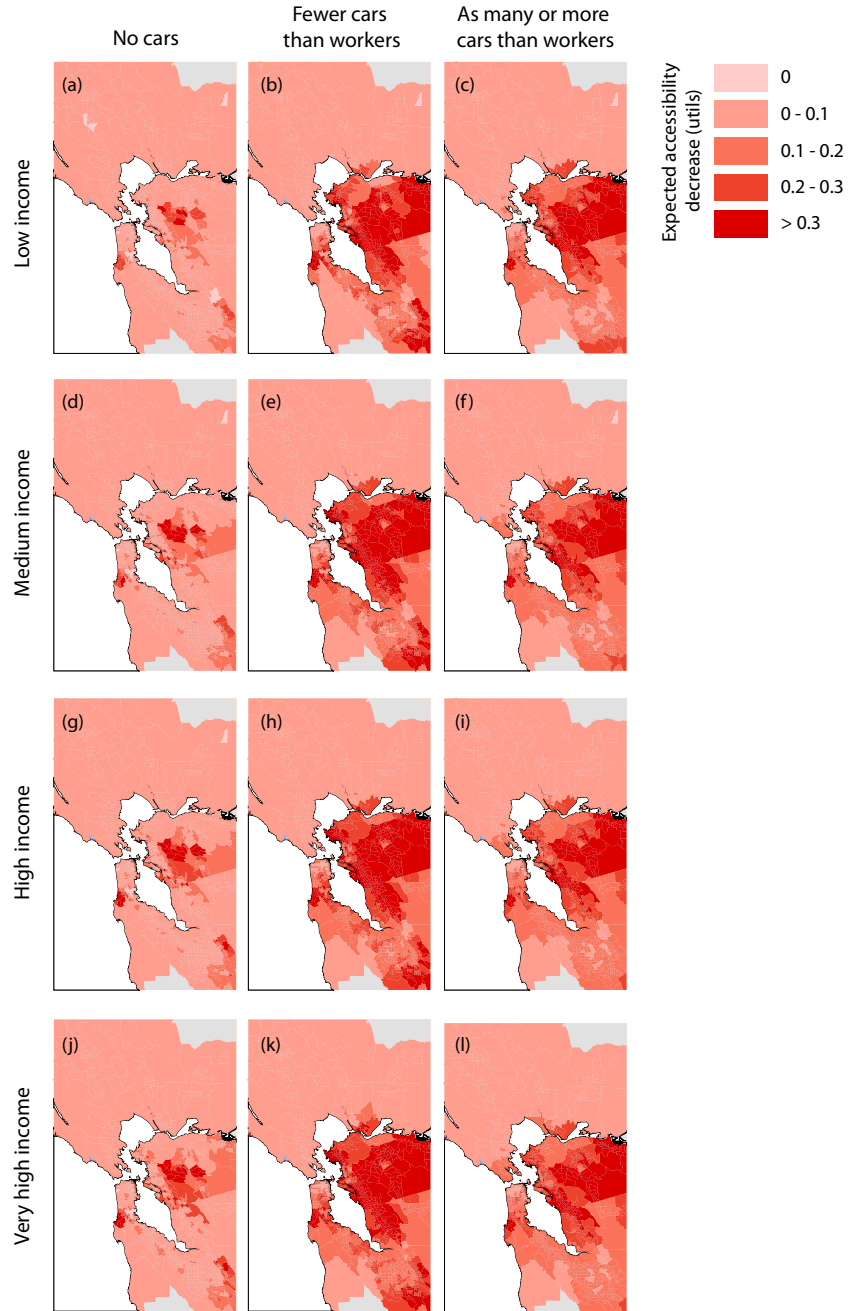


Figure 4: Expected changes in accessibility per person per day for each combination of income class and car ownership group. The darker the color, the greater the losses in accessibility. Each row of figures corresponds to an income class and each column corresponds to a class of car ownership).

to a higher expected decreases in accessibility (as seen by looking across a column in Figure 4). Households with more cars tend to take longer trips, and there is a relationship between needing to travel longer distances and needing an extra cars in a household. But there is only a weak

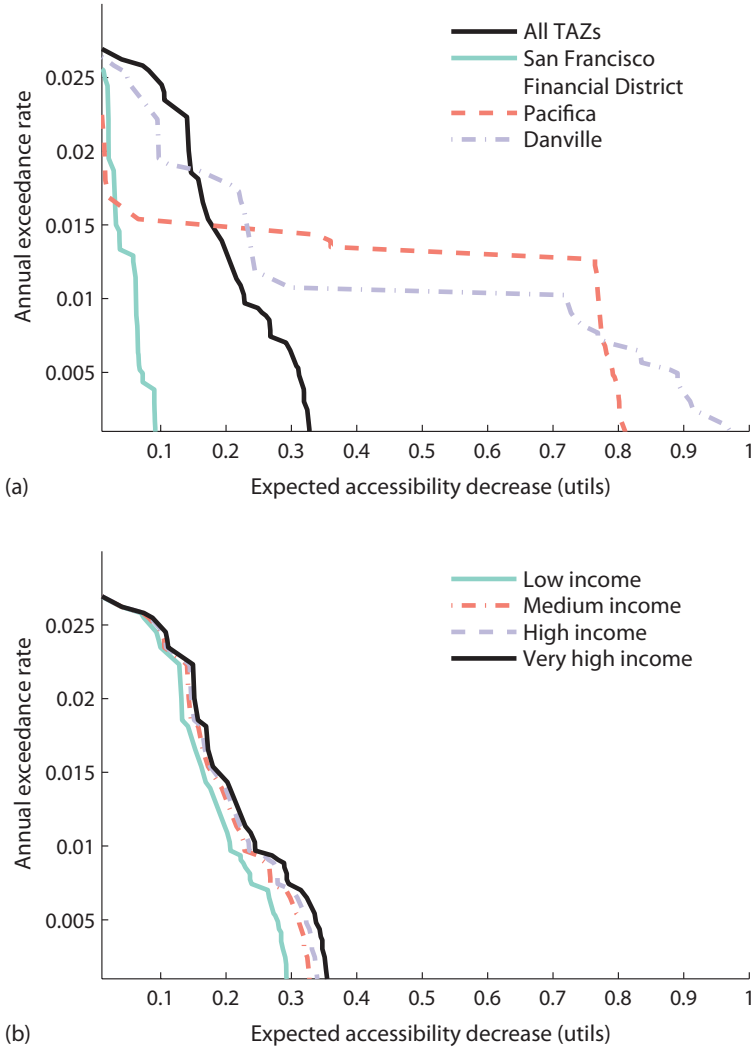


Figure 5: Accessibility annual loss exceedance curve with a comparison by (a) case study TAZs and average over all TAZs and (b) income class; all curves are for medium income households with fewer cars than workers.

trend between average trip length for a TAZ and the predicted impact on accessibility (Figure 6). Instead, we hypothesize that there are other latent variables correlated with both car ownership and accessibility risk (such as geographic location). In Section V, we will further explore the relationship between the percentage of car-based trips and accessibility risk.

Second, controlling for car ownership, we see a fairly consistent distribution of risk across income classes. For example, looking at households with fewer workers than cars (the middle column of Figure 4), the variation from TAZ to TAZ is much greater than the difference across income segments. Similarly, while trip lengths are slightly longer for higher income households, the differences are subtle. Thus, for a given TAZ, the differences in impacts across incomes are not that great. There is, however, an unequal geographic distribution of wealth in the study region.

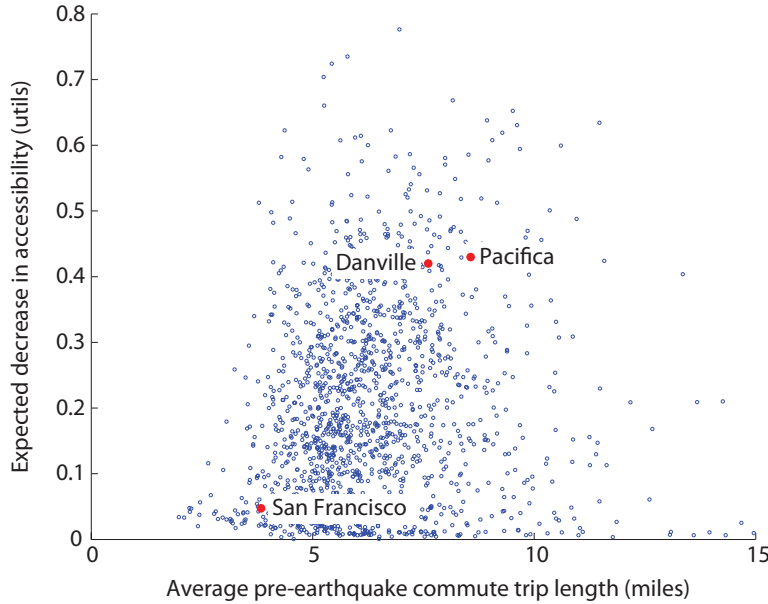


Figure 6: Average pre-earthquake trip length versus change in expected accessibility for all TAZs in the study region. Each dot represents data from one TAZ, and red dots highlight the data points for the three case study communities.

Because of this, when we aggregate accessibility risk across TAZs, we see that accessibility risk rises slightly with increasing household income (Figure 5b).

Next, we consider TAZs indicated to have elevated risk. The San Francisco Peninsula is at risk of disruption from large magnitude San Andreas earthquakes, while the East Bay is at risk from slightly smaller but more frequent events on the Hayward Fault. Network simulations indicate that both Hayward and San Andreas earthquakes can cause accessibility problems for the East Bay. Figure 7 shows realizations of a magnitude 6.85 Hayward event and a magnitude 7.45 San Andreas event—both show high accessibility losses in the East Bay. In contrast, the main predicted accessibility losses in San Francisco correspond primarily to San Andreas events. Figures 7c and 7d provide one such example. Figures 7e and 7f show a lower magnitude event farther away from the main population centers: a magnitude 6.35 event in the Great Valley Pittsburg-Kirby Hills Fault. This shows how the more minor faults in the East Bay can contribute to that area's risk. The Figure 7 results are for one specific socio-economic group, but comparable results for the other groups show the same patterns.

Finally, we can examine the rates of loss exceedance (eq. 4), as shown in Figure 5. Recognizing that the impact varies significantly by TAZ, as indicated by Figure 4, we also examine the accessibility loss exceedance curve for three communities: part of the San Francisco Financial District, Danville, and Pacifica. This part of the San Francisco Financial District represents an area with relatively low expected changes in accessibility, whereas Danville and Pacifica are at an elevated risk in almost all socio-economic groups (Figure 4). The general trends are corroborated by the loss exceedance curves for these three communities (Figure 5a shows results for medium income households with fewer cars than workers). The average middle-class person from Danville in a household with fewer cars than workers is expected to experience travel-related losses up to 1 util (or 75 minutes of extra travel time per day) after a rare earthquake. In contrast, a resident of San Francisco's Financial District has expected losses of only a tenth as much when considering

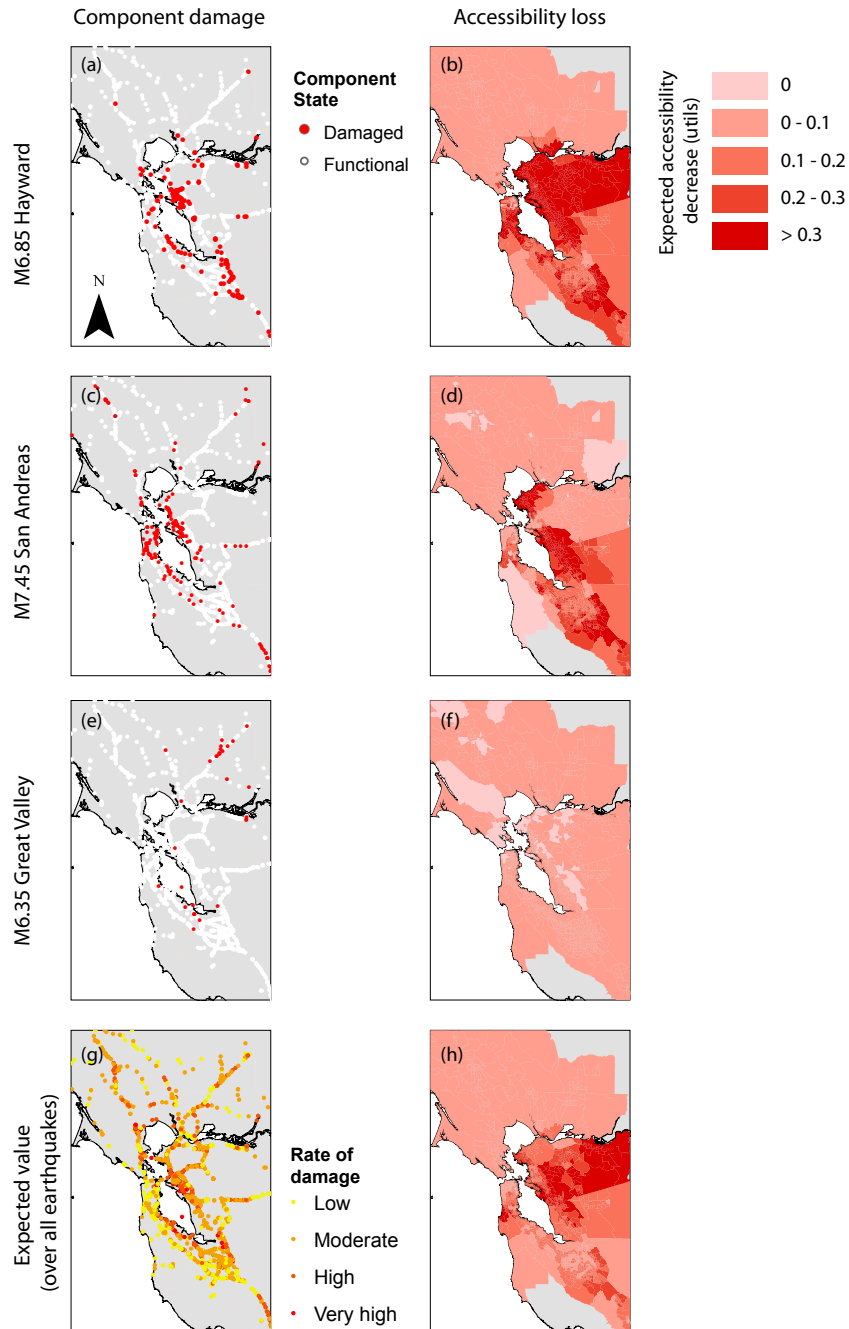


Figure 7: Bridge damage and corresponding accessibility losses by TAZ for medium income households with fewer cars than workers. The top three rows show results from specific events, while the bottom row has expected values calculated as a weighted average over all events.

320 the same exceedance rate. At annual rates of less than 0.01 (i.e., return periods greater than 100
 321 years), Danville and Pacifica follow a similar general pattern that differs dramatically from that of
 322 San Francisco.

323 II. Analysis for San Francisco Financial District

324 Two factors may explain this San Francisco TAZ's lower accessibility losses relative to most other
325 communities. First, it differs dramatically from many other TAZs in having a small percentage of
326 trips made by car (38% versus an average of 85% across all TAZs). Households traveling by foot
327 or bike are less influenced by network damage, because foot travel routes and travel times are
328 assumed to not be affected by bridge damage and road congestion. Additionally, trips by foot and
329 bike tend to be to destinations that are shorter distances away than trips made via other modes.
330 Second, the times for trips to and from work are similar to that of other TAZs, and the average trip
331 distance is only 7% lower than the average for all trips region-wide. So the trip times and lengths
332 do not explain the differences in accessibility losses in this TAZ. The data thus suggests that a
333 major cause for the low accessibility risk of this TAZ is the low dependence on cars for mobility.

334 III. Analysis for Pacifica

335 Pacifica is wedged between the Pacific Ocean to the west and the coastal mountains to the east. The
336 main access road is historic California Highway 1, which has a number of older and seismically
337 vulnerable bridges. There are no viable alternative routes to population centers via local roads.
338 Most trips from Pacifica are taken by car (88%), and the average trip length is 108% longer than
339 the region-wide average, so the Highway 1 vulnerability is particularly serious.

340 As a comparison, consider Half Moon Bay, a community about 13 miles to the South (Figure 8).
341 Half Moon Bay has significantly lower expected accessibility losses compared to Pacifica (0.11 *utils*
342 for a middle income household with fewer cars than workers, versus 0.43 *utils* in Pacifica). While
343 the seismic hazard for the two towns is similar, Half Moon Bay's population is about one third of
344 Pacifica's, so there is less local demand for Highway 1's limited road capacity [43]. Perhaps more
345 importantly, Half Moon Bay has a key alternative to California Highway 1: California Highway 92,
346 which links to the main highways of the peninsula. Since Pacifica is unusually reliant on one road
347 with key vulnerabilities, it has an elevated risk for losses in accessibility.

348 IV. Analysis for Danville

349 Danville is a suburban community with many residents commuting large distances by car. The
350 average length of a trip from Danville is 85% longer than the average over all trips in the study
351 region, with a relatively high proportion of trips taking more than 60 minutes and traveling over
352 40 miles. These longer trips have more opportunities to be impacted by road closures, because
353 more roads and bridges will be used to complete the trip. Moreover, many Danville trips are via
354 highways, which increases the likelihood of crossing (damage prone) highway bridges.

355 Bridge damage is important for many regions, including Danville, because the percentage
356 of car-based trips is high (85% of all trips from Danville, which is approximately average for
357 all TAZs). For all three simulations shown in Figure 7, some bridges in the Oakland area are
358 damaged and thus closed. In addition, in the first two simulations, there are closures to the north
359 of Danville, which represents one of the two main travel routes from Danville. There are also
360 scattered closed bridges to the west of Danville, a top travel corridor for people of Danville because
361 of the workplace centers in San Francisco, Oakland, and San Jose (all to the west). As for transit, in
362 the first two events, all BART lines are closed, so there are limited alternatives to the popular road
363 routes. The result is that the residents of Danville have reduced access to their normal destinations
364 after these events. Looking at the rate of bridge damage across all of the earthquake simulations
365 in Figure 7g, we see that bridges in the Oakland area and to the north of Danville are particularly

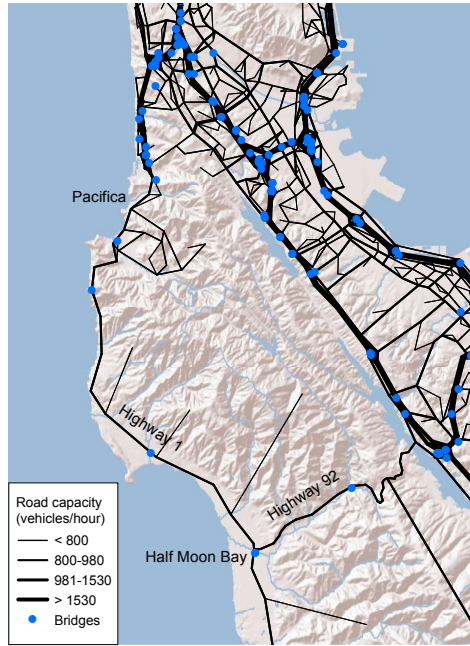


Figure 8: Roads providing access from Pacifica and Half Moon Bay.

likely to be damaged. This suggests that Danville's proximity to vulnerable bridges contributes to its accessibility risk.

368 V. Impact of travel mode shifts and regional variations in travel mode patterns

369 Over all the simulated events, taking a weighted average by the annual occurrence rate of each
 370 event, we see a 25% reduction in transit ridership after an earthquake. The heavy rail systems
 371 (BART and Caltrain) are not fully operational in most of the forty simulated events (Table 2),
 372 and these have heavy ridership. The light rail systems (VTA and Muni) also suffer losses in
 373 many events (Table 2). Some of the pre-earthquake transit trips do not take place at all in the
 374 post-earthquake simulations, and some switch to other modes (car, foot and bike), causing small
 375 average increases in the number of trips taken by other modes. One exception to this trend is the
 376 M6.35 Great Valley earthquake illustrated in Figure 7e and 7f. In this event, there were no line
 377 closures on the four major transit systems listed in Table 2. There were, however, some bridge
 378 closures on the highways, resulting in a slight increase in transit ridership and in trips by foot.

379 In general, accessibility impact grows with increasing number of damaged transit lines,
 380 particularly in combination with high numbers of damaged bridges (Figure 9). Individual network
 381 simulations also suggest that transit is a key contributor to accessibility risk. For example, the
 382 M6.85 Hayward and the M7.45 Northern San Andreas Fault events from Figure 7 both have around
 383 11% of bridges damaged. These events are labeled in Figure 9, which indicates that the Hayward
 384 event has significantly higher transit network damage and accessibility loss. The Northern San
 385 Andreas event had 10 of the 14 BART lines and all Muni lines operational, whereas the Hayward

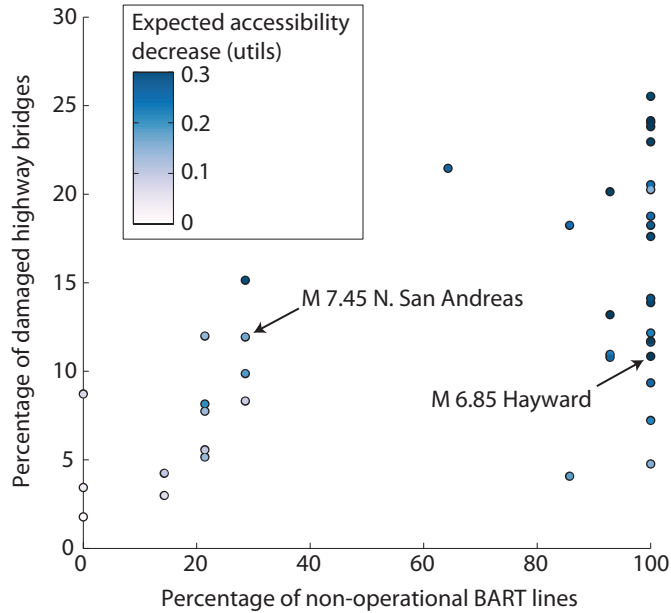


Figure 9: Percentage of BART lines not operational versus percentage of highway bridges damaged, where each data point corresponds to one earthquake simulation. The points are color-coded by the average loss in accessibility per day per person over all TAZs for households with the fewer cars than workers.

Table 2: Number of the 40 earthquake realizations in which for major transit networks have a specified level of functionality. Functionality is measured by the percentage of lines that are operational in a given realization.

Functionality	BART	Caltrain	Muni Light Rail	VTA Light Rail
Full	3	13	25	9
50-99%	10	0	15	0
1-49%	8	0	0	0
None	19	27	0	31

386 event had no BART lines and 5 of the 8 Muni lines operational (Caltrain and VTA were not
387 operational in either simulation). Moreover, the differences in accessibility results could not have
388 been predicted from simpler models focusing on bridge portfolio losses, because the percent of
389 damaged bridges was about the same, and the San Andreas event actually corresponded to a
390 greater increase in fixed-demand travel time when modeled using a much simpler traffic model.

391 Next, we examine the correlation between a community's walkability, as measured by the
392 percentage of total trips made by that travel mode, and its expected decrease in accessibility.
393 Figure 10 shows that communities with a high percentage of pre-earthquake trips on foot have
394 a lower average decrease in accessibility. This result corroborates the specific example of the
395 San Francisco Financial District discussed in Section II. Furthermore, on average, the number
396 of by-foot trips increases after the earthquake events where road congestion worsens. This
397 model result is consistent with the observations after the 1995 Kobe earthquake, in which many
398 commuters switched to walking and biking in the weeks after the earthquake [7]. This suggests
399 that communities with greater walkability are also more resilient to earthquake-related accessibility
400 risk.

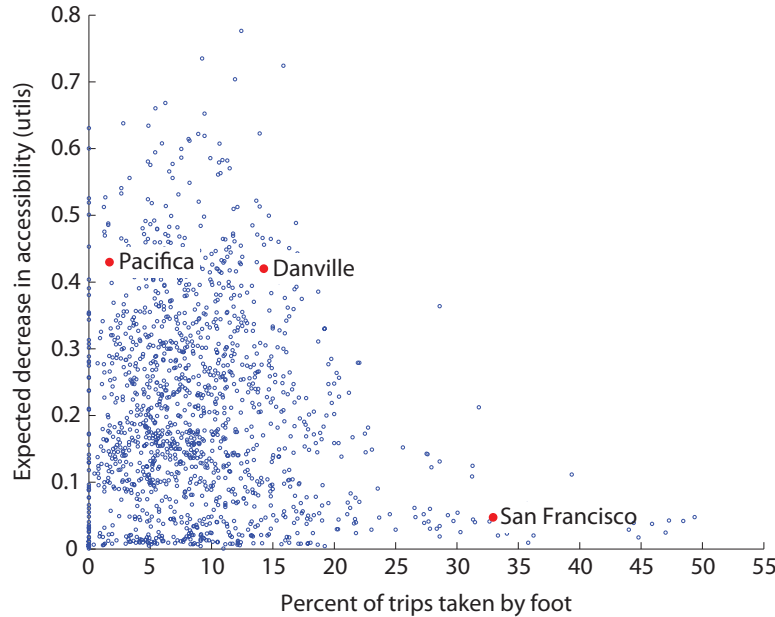


Figure 10: Percentage of pre-earthquake trips taken by foot versus expected decrease in accessibility among households with fewer cars than workers, for all TAZs in the study area. Each dot represents data from one TAZ, and red dots highlight the data points for the three case study communities.

401

IV. CONCLUSIONS

402 We have shown how mode-destination accessibility can be used to link post-earthquake infra-
 403 structure damage to the impact on human welfare and enables identifying at-risk geographic and
 404 demographic groups in a region. Adopting this performance metric from the urban planning
 405 community, we have illustrated its use for seismic risk assessment and mitigation through a case
 406 study of the San Francisco Bay Area. For the case study, we considered a set of 40 hazard-consistent
 407 earthquake scenarios, ground-motion intensity maps, damage maps, and corresponding annual
 408 rates of occurrence. For each damage map, we performed a detailed activity-based travel model
 409 calculation that includes the road network, transit networks, walking and biking options, variable
 410 travel demand, and mode choice. We used this data and model to compute the mode-destination
 411 accessibility, a performance measure for each community and each socio-economic group (defined
 412 by income class and car ownership). This procedure is more resource intensive than a more trad-
 413 itional approach of considering impacts from a single disaster scenario, but it provides additional
 414 insight by providing a complete characterization of the uncertain future impacts of earthquakes.
 415 For example, the case study region is known to be vulnerable to future San Andreas or Hayward
 416 fault ruptures, which are frequently used for planning purposes in the area, but this study showed
 417 that some regions in the East Bay are at great risk from other less-widely-considered rupture
 418 scenarios.

419 We saw stark differences in accessibility from location to location. We found that these
 420 geographic trends persisted across income classes and car ownership groups. Nonetheless, higher
 421 income households with more cars than workers had higher average accessibility losses than other
 422 socio-economic groups. One reason for this is the geographic clustering of these households in
 423 higher-risk areas. Another factor is that these households tend to take longer daily trips, thus
 424 crossing more roads and bridges and possibly increasing the likelihood of disruption. We also

425 considered three specific communities that were predicted to have greatly differing experiences
426 after a future earthquake, in order to understand the geographic and demographic reasons
427 underlying these differences in risk.

428 This study considered the possibility that travel modes will shift after an earthquake, and
429 communities that can more easily adjust are predicted to experience lower post-earthquake losses
430 in accessibility. The results suggest that the walkability of a community, as measured by the
431 percentage of pre-earthquake trips by foot, is closely linked to reduced accessibility risk. We also
432 found that in almost all of the simulated earthquake events, the transit system is predicted by
433 this model to be severely impacted. The result is a reduced mode share for transit and increased
434 trips by other modes (car, walking, and bike). Thus, this study suggests that neglecting to
435 consider transit disruption can lead to a nonconservative estimate of seismic risk of transportation
436 systems. The model shows, however, that when transit is not damaged—which is rare for this case
437 study—ridership increases. As impacts of these system characteristics are better identified, the
438 proposed approach can provide a benchmark against which potential simplified decision-making
439 approaches can be evaluated.

440 In conclusion, mode-destination accessibility offers important insights into the relationship
441 between damage to physical infrastructure and impacts on human welfare. Using a detailed
442 transportation network model, computationally efficient analysis strategies, and this refined
443 measure of impact, we obtain new insights about users' risk, and obtain metrics that are usable by
444 urban planners responsible for long-term management of transportation systems. This approach
445 provides a foundation for future work in risk mitigation and policy to reduce the vulnerability of
446 at-risk communities. It suggests that initiatives making communities more conducive for cycling
447 and walking to work can increase resiliency to disasters. It also provides a method to quantify
448 economic and societal benefits of upgrading various aspects of a region's transportation systems.

449

V. ACKNOWLEDGEMENTS

450 We thank Dave Ory at the Metropolitan Transportation Commission (MTC) and Tom Shantz and
451 Loren Turner at Caltrans for motivating discussions and providing the case study data. The first
452 author thanks the support of the NSF and Stanford Graduate Research Fellowships. This work was
453 supported in part by the National Science Foundation under NSF grant number CMMI 0952402.
454 Any opinions, findings and conclusions or recommendations expressed in this material are those
455 of the authors and do not necessarily reflect the views of the National Science Foundation.

456

REFERENCES

- 457 [1] L. Dueñas-Osorio, J. I. Craig, B. J. Goodno, Seismic response of critical interdependent
458 networks, *Earthquake Engineering & Structural Dynamics* 36 (2) (2007) 285–306. doi:10.
459 1002/eqe.626.
- 460 [2] S. E. Chang, M. Shinozuka, J. E. Moore, Probabilistic earthquake scenarios: Extending risk
461 analysis methodologies to spatially distributed systems, *Earthquake Spectra* 16 (3) (2000)
462 557–572. doi:10.1193/1.1586127.
- 463 [3] R. C. Bolin, L. Stanford, *The Northridge earthquake: vulnerability and disaster*, Routledge,
464 London; New York, 1998.
- 465 [4] The World Bank and the United Nations, *Natural hazards, unnatural disasters: the economics*
466 *of effective prevention*, Tech. rep., The World Bank, Washington D.C. (2010).

- 467 [5] California. Dept. of Transportation. Post Earthquake Investigation Team, Northridge earth-
468 quake, 17 January 1994: PEQIT report, California Department of Transportation, Division of
469 Structures, Sacramento, 1994.
- 470 [6] K. J. Tierney, Business Impacts of the Northridge Earthquake, *Journal of Contingencies and*
471 *Crisis Management* 5 (2) (1997) 87–97. doi:10.1111/1468-5973.00040.
- 472 [7] P. Gordon, H. W. Richardson, B. Davis, Transport-related impacts of the Northridge earth-
473 quake, National Emergency Training Center, 1998.
- 474 [8] A. Kiremidjian, J. Moore, Y. Y. Fan, O. Yazlali, N. Basöz, M. Williams, Seismic risk assessment
475 of transportation network systems, *Journal of Earthquake Engineering* 11 (3) (2007) 371–382.
476 doi:10.1080/13632460701285277.
- 477 [9] N. Jayaram, J. W. Baker, Efficient sampling and data reduction techniques for probabilistic
478 seismic lifeline risk assessment, *Earthquake Engineering & Structural Dynamics* 39 (10) (2010)
479 1109–1131. doi:10.1002/eqe.988.
- 480 [10] C. S. Oliveira, M. A. Ferreira, F. M. d. Sá, The concept of a disruption index: application to the
481 overall impact of the July 9, 1998 Faial earthquake (Azores islands), *Bulletin of Earthquake*
482 *Engineering* 10 (1) (2012) 7–25. doi:10.1007/s10518-011-9333-8.
- 483 [11] P. Bocchini, D. M. Frangopol, Restoration of bridge networks after an earthquake: Multicri-
484 teria intervention optimization, *Earthquake Spectra* 28 (2) (2012) 426–455. doi:10.1193/1.
485 4000019.
- 486 [12] F. Cavalieri, P. Franchin, P. Gehl, B. Khazai, Quantitative assessment of social losses based
487 on physical damage and interaction with infrastructural systems, *Earthquake Engineering &*
488 *Structural Dynamics* 41 (11) (2012) 1569–1589. doi:10.1002/eqe.2220.
- 489 [13] F. S. Chapin, *Urban land use planning*, University of Illinois Press, 1970.
- 490 [14] D. A. Niemeier, Accessibility: an evaluation using consumer welfare, *Transportation* 24 (4)
491 (1997) 377–396.
- 492 [15] K. T. Geurs, B. van Wee, Accessibility evaluation of land-use and transport strategies: review
493 and research directions, *Journal of Transport Geography* 12 (2) (2004) 127–140. doi:10.1016/
494 j.jtrangeo.2003.10.005.
- 495 [16] S. L. Handy, D. A. Niemeier, Measuring accessibility: an exploration of issues and alternatives,
496 *Environment and Planning A* 29 (7) (1997) 1175–1194.
- 497 [17] M. Miller, Seismic risk assessment of complex transportation networks, PhD thesis, Stanford
498 University (2014).
- 499 [18] M. Miller, J. Baker, Ground-motion intensity and damage map selection for probabilistic infras-
500 tructure network risk assessment using optimization, *Earthquake Engineering & Structural*
501 *Dynamics* (2014). doi:10.1002/eqe.2506.
- 502 [19] R. Cervero, K.-L. Wu, Polycentrism, commuting, and residential location in the San Francisco
503 Bay area, *Environment and Planning A* 29 (5) (1997) 865–886.
- 504 [20] Y. Han, R. A. Davidson, Probabilistic seismic hazard analysis for spatially distributed
505 infrastructure, *Earthquake Engineering & Structural Dynamics* 41 (15) (2012) 2141–2158.
506 doi:10.1002/eqe.2179.

- 507 [21] E. H. Field, T. H. Jordan, C. A. Cornell, OpenSHA: a developing community-modeling
508 environment for seismic hazard analysis, *Seismological Research Letters* 74 (4) (2003) 406 –
509 419. doi:10.1785/gssrl.74.4.406.
- 510 [22] M. Shinozuka, Y. Murachi, X. Dong, Y. Zhou, M. J. Orlikowski, Effect of seismic retrofit of
511 bridges on transportation networks, *Earthquake Engineering and Engineering Vibration* 2 (2)
512 (2003) 169–179. doi:10.1007/s11803-003-0001-0.
- 513 [23] E. H. Field, T. E. Dawson, K. R. Felzer, A. D. Frankel, V. Gupta, T. H. Jordan, T. Parsons,
514 M. D. Petersen, R. S. Stein, R. J. Weldon, C. J. Wills, Uniform California Earthquake Rupture
515 Forecast, Version 2 (UCERF 2), *Bulletin of the Seismological Society of America* 99 (4) (2009)
516 2053 –2107. doi:10.1785/0120080049.
- 517 [24] D. J. Wald, T. I. Allen, Topographic slope as a proxy for seismic site conditions and
518 amplification, *Bulletin of the Seismological Society of America* 97 (5) (2007) 1379–1395.
519 doi:10.1785/0120060267.
- 520 [25] D. M. Boore, G. M. Atkinson, Ground-motion prediction equations for the average horizontal
521 component of PGA, PGV, and 5%-damped PSA at spectral periods between 0.01 s and 10.0 s,
522 *Earthquake Spectra* 24 (1) (2008) 99–138.
- 523 [26] N. Jayaram, J. W. Baker, Correlation model for spatially distributed ground-motion intensities,
524 *Earthquake Engineering & Structural Dynamics* 38 (15) (2009) 1687–1708. doi:10.1002/eqe.
525 922.
- 526 [27] N. Basöz, J. Mander, Enhancement of the highway transportation lifeline module in HAZUS,
527 Tech. rep., Final Pre-Publication Draft (#7) prepared for the National Institute of Building
528 Sciences (NIBS) (1999).
- 529 [28] K. N. Ramanathan, Next generation seismic fragility curves for California bridges incorporating
530 the evolution in seismic design philosophy, PhD thesis, Georgia Institute of Technology
531 (2012).
- 532 [29] S. Werner, C. Taylor, S. Cho, J. Lavoie, REDARS 2 methodology and software for seismic risk
533 analysis of highway systems (technical manual), Tech. rep., Seismic Systems & Engineering
534 Analysis for MCEER, Oakland, CA (2006).
- 535 [30] Caltrans, Caltrans Seismic Design Criteria Version 1.7, Tech. Rep. SDC 1.7, California Depart-
536 ment of Transportation, Sacramento, CA (2013).
- 537 [31] Bechtel/HNTB Team, Design Criteria Volume I, Version 1.2, Tech. rep., San Francisco Bay
538 Area Rapid Transit District, San Francisco Bay Area Rapid Transit District Earthquake Safety
539 Program (2008).
- 540 [32] N. Kurtz, J. Song, P. Gardoni, Time-varying seismic reliability analysis of representative US
541 west coast bridge transportation networks, in: G. Deodatis, B. R. Ellingwood, D. M. Frangopol
542 (Eds.), *Safety, Reliability, Risk and Life-Cycle Performance of Structures and Infrastructures*,
543 CRC Press, 2014, pp. 655–662.
- 544 [33] J. Ghosh, K. Roknuddin, J. E. Padgett, L. Dueñas-Osorio, Seismic reliability assessment of
545 aging highway bridge networks with field instrumentation data and correlated failures. I:
546 Methodology, *Earthquake Spectra* 30 (2) (2013) 795–817. doi:10.1193/040512EQS155M.

- 547 [34] K. Kockelman, Travel Behavior as Function of Accessibility, Land Use Mixing, and Land Use
548 Balance: Evidence from San Francisco Bay Area, *Transportation Research Record: Journal of*
549 *the Transportation Research Board* 1607 (-1) (1997) 116–125. doi:10.3141/1607-16.
- 550 [35] P. Waddell, F. Nourzad, Incorporating nonmotorized mode and neighborhood accessibility in
551 an integrated land use and transportation model system, *Transportation Research Record: Journal of*
552 *the Transportation Research Board* 1805 (-1) (2002) 119–127. doi:10.3141/1805-14.
- 553 [36] C. F. Manski, *Structural analysis of discrete data with econometric applications*, MIT Press,
554 1981.
- 555 [37] K. A. Small, H. S. Rosen, Applied welfare economics with discrete choice models, *Economet-
556 rica* 49 (1) (1981) 105–130. doi:10.2307/1911129.
- 557 [38] D. Ory, Personal communication (2013).
- 558 [39] United States Department of Transportation, Revised departmental guidance: valuation of
559 travel time in economic analysis, US Department of Transportation, Washington, DC.
- 560 [40] G. Erhardt, P. Brinckerhoff, D. Ory, A. Sarvepalli, J. Freedman, J. Hood, B. Stabler, MTC's
561 Travel Model One: applications of an activity-based model in its first year, in: *Innovations in*
562 *Travel Modeling 2012*, Tampa, Florida, 2012, p. 9.
- 563 [41] P. Waddell, UrbanSim: modeling urban development for land use, transportation, and
564 environmental planning, *Journal of the American Planning Association* 68 (3) (2002) 297–314.
565 doi:10.1080/01944360208976274.
- 566 [42] W. Davidson, P. Vovsha, J. Freedman, R. Donnelly, CT-RAMP family of activity-based models,
567 in: *Proceedings of the 33rd Australasian Transport Research Forum (ATRF)*, Canberra,
568 Australia, 2010, p. 15.
- 569 [43] U.S. Bureau of the Census, United States Census 2010, Tech. rep., U.S. Census Bureau,
570 Washington D.C. (2010).